Antiblockade in Rydberg Excitation of an Ultracold Lattice Gas

C. Ates,[1] T. Pohl,[2] T. Pattard,[1] and J. M. Rost[1]

[1]*Max Planck Institute for the Physics of Complex Systems, Nöthnitzer Straße 38, D-01187 Dresden, Germany*
[2]*ITAMP, Harvard-Smithsonian Center for Astrophysics, 60 Garden Street, Cambridge, Massachusetts 02138, USA*

(Received 12 May 2006; published 8 January 2007)

It is shown that the two-step excitation scheme typically used to create an ultracold Rydberg gas can be described with an effective two-level rate equation, greatly reducing the complexity of the optical Bloch equations. This allows us to efficiently solve the many-body problem of interacting cold atoms with a Monte Carlo technique. Our results reproduce the observed excitation blockade effect. However, we demonstrate that an Autler-Townes double peak structure in the two-step excitation scheme, which occurs for moderate pulse lengths as used in the experiment, can give rise to an antiblockade effect. It is most pronounced for atoms arranged on a lattice. Since the effect is robust against a large number of lattice defects it should be experimentally realizable with an optical lattice created by CO_2 lasers.

DOI: 10.1103/PhysRevLett.98.023002 PACS numbers: 32.70.Jz, 32.80.Rm, 34.20.Cf

Because of the strong interactions between highly excited Rydberg atoms, laser excitation of cold atomic gases to such states substantially differs from what is known for low excitations or isolated atoms. In the extreme case of very dense atomic samples, multiple excitations may even be completely suppressed, such that the gas acts as a single ''superatom''. This effect was first proposed to create mesoscopic devices for quantum information processing [1] and has sparked several experiments [2–4] which demonstrated a partial excitation blockade effect. Beyond potential applications in quantum information, the correlated dynamics of cold gases, manifest in this excitation suppression, poses an interesting and conceptually challenging [2,5] many-body problem since the numerical effort to solve it increases exponentially with the number of atoms rendering a full quantum treatment of realistically large systems presently intractable.

Here, we describe an approach which allows for an efficient treatment of very large systems, while still covering the highly correlated nature of the gas dynamics. The approach is applicable under well-defined conditions which are realized, e.g., in the two-step excitation schemes of [3,4]. We can reproduce the observed excitation blockade as well as its effect on the atom counting statistics [6], as observed in [4]. However, in addition we predict the opposite effect, namely, an interaction-induced excitation enhancement or ''antiblockade''. It is most pronounced for a lattice gas and may even be used to gain quantitative information about the strength of interaction between Rydberg atoms.

While in [2] Rydberg excitations to principal quantum numbers $n = 30$–80 are achieved by a single photon of a pulsed UV laser from the $5s$ Rb ground state, in [3,4] a two-step scheme is used where a strong pump laser drives the $5s$-$5p$ transition of Rb atoms and a tunable second laser excites Rydberg atoms from the $5p$ state. In all three experiments a suppression of the excitation has been observed as a function of increasing laser intensity or/and density of the gas. However, as the two excitation schemes are very different in nature, they may lead to dramatic differences in the excitation dynamics of the system. In fact, as we will show, the two-step scheme can induce an antiblockade due to a transient Autler-Townes splitted shape of the *single-atom* excitation probability $P_e(t, \Delta)$ as a function of the detuning Δ from resonance.

In the two-step excitation of a three-level system the initial state $|g\rangle$ (typically the ground state) and the Rydberg state $|e\rangle$ are optically coupled to an intermediate state $|m\rangle$ (see Fig. 1). The Rabi frequency Ω of the lower transition is typically much larger than the Rabi frequency ω of the Rydberg excitation. Moreover, the intermediate level $|m\rangle$ decays with a rate $\Gamma \gg \omega$, large compared to the upper Rabi frequency ω. Under these conditions, i.e., $\Omega \gg \omega$, $\Gamma \gg \omega$ and for a Rydberg excitation pulse longer than Γ^{-1} one can adiabatically eliminate all coherences and the population of the intermediate state [7] in the optical Bloch equations [8], which ultimately reduce to a linear rate equation

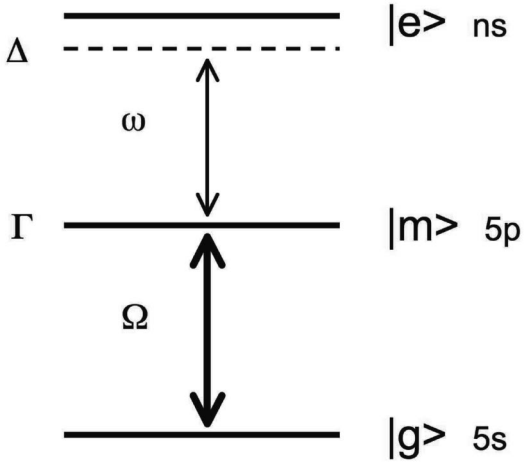

FIG. 1. Sketch of the two-step excitation scheme.

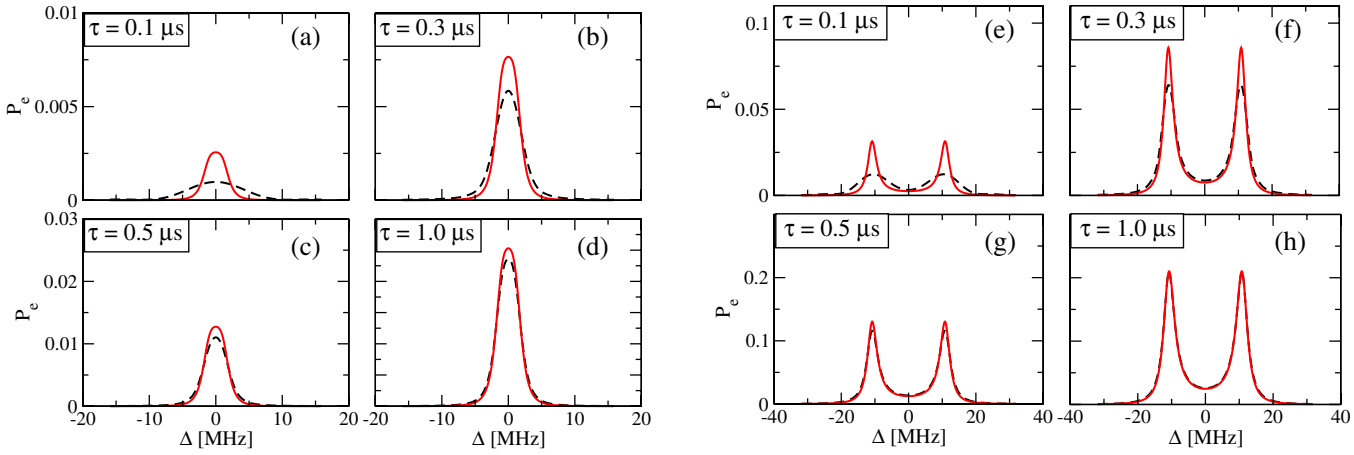

FIG. 2 (color online). The population P_e of the Rydberg state $|e\rangle$ in the three-level system of Fig. 1 according to the equation (2) (solid) and the optical Bloch equation (dashed) for different pulse lengths τ. The parameters are $\Omega = 4$, $\omega = 0.2$, $\Gamma = 6$ MHz for the left set (a)–(d) and $\Omega = 22.1$, $\omega = 0.8$, $\Gamma = 6$ MHz for the right set (e)–(h).

$$\dot{P}_e = \gamma(1 - P_e) - \gamma_\downarrow P_e \tag{1}$$

of an effective two-level system for the Rydberg state population $P_e(t)$, where γ and $\gamma_\downarrow$ denote the excitation and deexcitation rate, respectively. Solving Eq. (1) yields

$$P_e(t, \Delta) = P_\infty(\Delta)\left(1 - \exp\left[-\frac{\gamma(\Delta)t}{P_\infty(\Delta)}\right]\right), \tag{2}$$

where $P_\infty = P_e(t \to \infty, \Delta)$ is the steady-state occupation of $|e\rangle$. For typical Rabi frequencies [3,4] and pulse lengths of $\tau \geq 0.5$ μs, the excitation is well described by Eq. (2) and has the intuitively expected resonance shape with a single peak [Figs. 2(a)–2(d)]. However, also a double peak structure with maxima at finite detuning Δ [Figs. 2(e)–2(h)] can occur. The latter is due to the Autler-Townes splitting of the intermediate state $|m\rangle$ under strong driving of the $|m\rangle \leftrightarrow |g\rangle$ transition.

Adding a second Rydberg atom the detuning Δ is given by the sum of the laser detuning and the interaction-induced shift of the atomic transition frequency. In general, the interaction between two Rydberg atoms can be rather complicated, due to the mixing of a large number of electronically excited molecular potential curves. However, as demonstrated in [9], a simplified treatment, which for a given atom pair neglects the couplings to all but the energetically closest two-atom state, provides a very good description of the interatomic potential at large distances r. Consider a pair of Rb atoms in an $[ns, ns]$ state coupled to a pair of atoms in state $[np, (n-1)p]$ by the interaction term, $V(r) = \mu_{sp}\mu_{sp'}/r^3$. Here, the dipole moments μ_{sp} and $\mu_{sp'}$ represent the $ns \to np$ and $ns \to (n-1)p$ transitions, respectively. Since the dipole coupling to the $[p, p']$ pair is off resonant by $\delta_0 < 0$, the resulting potential, connected to the (ns, ns) asymptote, is repulsive and reads [10]

$$\delta(r) = \frac{1}{2}(\delta_0 + \sqrt{\delta_0^2 + 4V^2}). \tag{3}$$

Proceeding to N atoms, we note that the energy shift for the Rydberg state of an atom at r_j is now given by the sum of shifts induced by all existing Rydberg atoms at positions $\mathbf{r}_i$ in the gas, $\Delta_j = \sum_{i \neq j} \delta(|\mathbf{r}_i - \mathbf{r}_j|)$. These shifts determine individual rates $\gamma_{(\downarrow)}(\Delta_j)$ for (de-)excitation of each atom which enter a many-body rate equation. While still describing the complete set of many-body states, which increases exponentially with the number of atoms, it can be efficiently solved within a standard Monte Carlo procedure. This allows us to treat large systems with several 10^5 atoms.

Figure 3 shows the calculated dependence of the fraction of Rydberg atoms f_e on the degree of excitation n for laser parameters similar to those of the experiment [3] but for

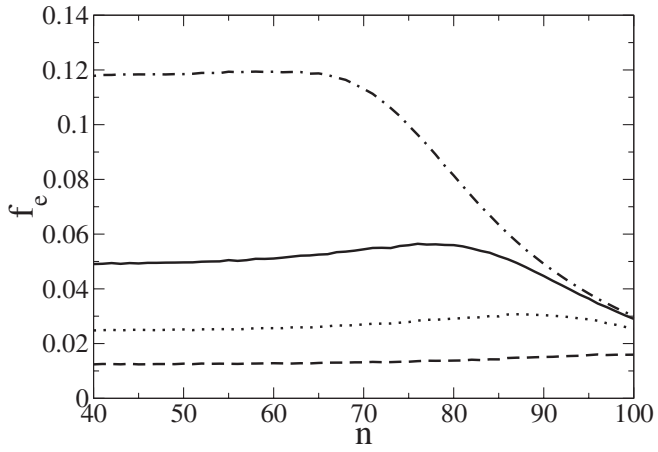

FIG. 3. The fraction of Rydberg atoms f_e as a function of increasing excitation n and for laser pulse lengths of 0.5 (dashed line), 1 (dotted line), 2 (solid line), and 5 μs (dotted-dashed line). The density of the ultracold gas is $\rho = 8 \times 10^9$ cm^{-3}, and the laser parameters are $\Omega = 22.1$, $\omega = 0.8$, $\Gamma = 6$ MHz.

pulse lengths $\tau \leq 5$ μs considerably shorter than the 20 μs in the experiment. At shorter pulse lengths plasma formation due to ionizing atom-atom collisions does not play a role, since for repulsive interactions as considered here, ionization is greatly suppressed [9]. It is further reduced in the spatially ordered systems, discussed below.

As in the experiments, Fig. 3 reveals that the blockade effect is stronger for longer pulses. In fact long pulses completely mask the antiblockade effect (curve for $\tau = 5$ μs), which manifests itself in a nonmonotonic behavior of f_e with a slight initial increase (curves for $\tau < 5$ μs in Fig. 3). The antiblockade is weak since the distribution of interatomic distances in the gas does not allow for a large excitation enhancement at a specific interaction strength.

The Autler-Townes splitting, however, leads to a drastic effect for regularly spaced atoms, as demonstrated in Fig. 4 for a simple cubic lattice with a lattice constant of $a = 5$ μm. Restricting the distribution of interatomic distances leads to a resonant excitation enhancement for certain values of n. The position and shape of the peaks is readily understood by analyzing the geometry of the atoms on the cubic lattice.

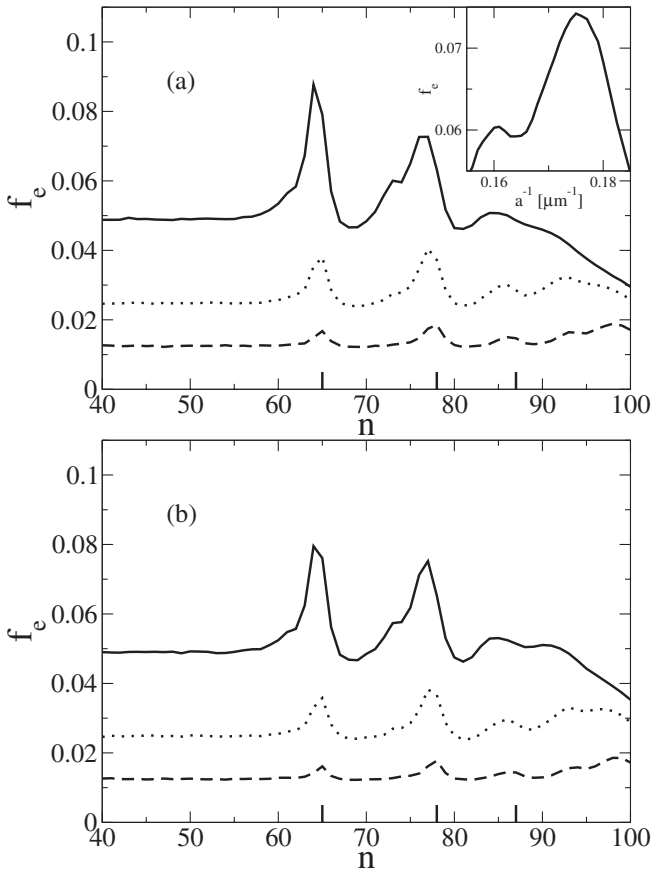

FIG. 4. The fraction of excited Rydberg atoms f_e as a function of increasing excitation n for atoms regularly arranged in a three-dimensional simple cubic lattice with lattice constant 5 μm ($\rho = 8 \times 10^9$ cm^{-3}) and parameters as in Fig. 3; (a) perfect filling of lattice sites, (b) 20% lattice defects (i.e., empty lattice sites). The inset in (a) shows the peak of f_e corresponding to atom spacing a_2 (see text) as function of the inverse lattice constant a^{-1} at $n = 82$ and $\tau = 2$ μs.

The interaction shift of the Rydberg transition of a given atom is dominantly induced by Rydberg atoms located at closest possible distances a_j. For a simple cubic lattice they are given by $a_j = \sqrt{j}a$, corresponding to nearest neighbors (a_1), neighbors along the diagonal (a_2), and those along the cubic diagonal (a_3). The excitation probability reaches a maximum if the corresponding shift $\delta(a_j; n_j)$ for a given quantum number n_j matches the position Δ_m of the Autler-Townes peaks of the single-atom spectrum (Fig. 2). This leads to the peaks in Fig. 4. Their position is determined by

$$\delta(a_j; n_j) = \Delta_m, \tag{4}$$

which for the parameters of Fig. 4 predicts $\{n_1, n_2, n_3\} = \{65, 78, 87\}$, in good agreement with the numerical values of $\{65, 77, 86\}$ for the shortest pulse length of 0.5 μs. Compared to Eq. (4) the peak positions are only slightly shifted towards lower n, due to the presence of other, more distant Rydberg atoms in addition to the nearest neighbor. Hence, varying the lattice spacing and the Rabi frequencies, i.e., the Autler-Townes splitting, Eq. (4) provides an accurate relation to experimentally probe the long-range part of Rydberg atom interaction over a wide range of excited states.

The position of the main peaks is due to two-atom interactions. Three-particle correlations, which correspond to two Rydberg atoms equally contributing to the interaction shift of the Rydberg transition of an atom located between them, give rise to additional structures, see Fig. 4. They form at the low-n side of the main peaks since the corresponding resonance condition requires a weaker single-atom shift. Because of the limited resolution in n, the additional excitation enhancements are difficult to identify in $f_e(n)$, but clearly appear as side peaks when f_e is probed as a function of the inverse mean atomic spacing $a^{-1} \equiv \rho^{1/3}$ at constant n [inset of Fig. 4(a)].

A lattice with characteristic spacing of $a \sim 5$ μm can be produced by CO_2 lasers [11], but perfect filling of the lattice is difficult to achieve experimentally. Therefore, we have also studied the influence of random lattice defects. As shown in Fig. 4(b), even 20% of defects hardly diminishes the contrast of the excitation enhancement, since it relies dominantly on contributions from pairs of close neighbors; i.e., a missing neighbor due to a lattice defect leads neither to an antiblockade nor a blockade and therefore does not spoil f_e. This robustness of the observed peak structure makes an experimental verification of the antiblockade feasible, leaving the realization of the double peak structure in the single-atom excitation spectrum as the most crucial experimental constraint.

For typical laser parameters, the splitting of the single-atom excitation probability is only a transient effect, such that the appearance of the antiblockade peaks also depends on the length τ of the Rydberg excitation pulse. Figure 5 illustrates the corresponding boundary between the single

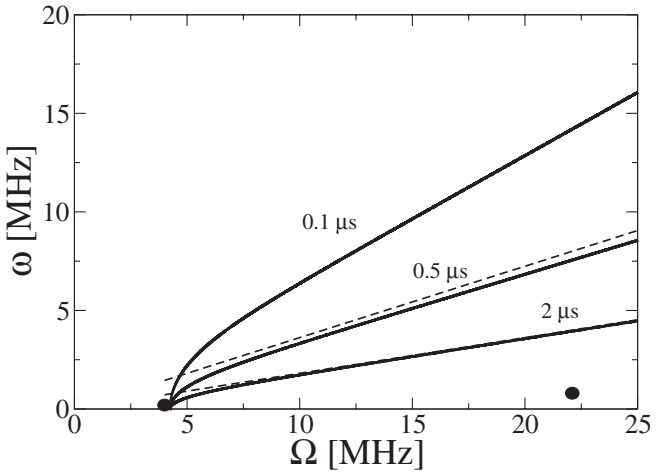

FIG. 5. Boundary in ω-Ω space between the blockade (upper area) and the antiblockade (lower area) regime for different pulse lengths and fixed $\Gamma = 6$ MHz. The dashed lines are the linear approximations for $\Omega \gg \omega$, see text. The parameters of Fig. 2 are indicated by black dots.

peak (blockade) and double peak (antiblockade) domain for different values of τ. For large τ, the exponential term in Eq. (2) is suppressed and the steady-state probability P_∞ dominates, resulting in a single peak [12]. On the other hand, for small $\gamma\tau/P_\infty$ the Rydberg population is governed by γ, which gives rise to the Autler-Townes splitting in P_e. The rate γ, as well as P_∞, take on a relatively simple form in the limit $\omega \ll \Gamma \ll \Omega$,

$$\gamma = \frac{\Gamma\omega^2/\Omega^2}{2(1 - 4\Delta^2/\Omega^2)^2}, \qquad P_\infty = \frac{1}{1 + 8\Delta^2/\Omega^2}. \quad (5)$$

From $\partial^2 P_e(\tau, \Delta)/\partial\Delta^2|_{\Delta=0} = 0$ and Eq. (5) we obtain a universal condition for the transition from the double to the single peak structure of $P_e(\tau, \Delta)$, which can be written as

$$g_0 = 2\ln(1 + g_0) = 2.513, \quad (6)$$

with $g_0 = \Gamma\tau\omega^2/\Omega^2$. Hence, for $\Omega \gg \omega$ the two regimes are separated by a linear boundary of $\omega = \alpha\Omega$, where $\alpha^2 = g_0/(\tau\Gamma)$ (see dashed lines in Fig. 5). Note also, that Eq. (5) clearly demonstrates the transient character of the double peak structure which vanishes for long laser pulses. Yet, experimentally accessible parameters, as, e.g., in [3], realize exactly the transient regime and therefore provide the conditions to see the antiblockade.

To summarize, we have derived a rate equation for the population of Rydberg states in ultracold gases produced in a two-step excitation scheme. The rate describes very well the structure of the Rydberg excitation in a single atom when compared to the exact solution of the Bloch equations including a transient Autler-Townes splitting in the Rydberg population for certain parameters.

The validity of the rate equation has allowed us to formulate an efficient Monte Carlo treatment of the correlated many-body excitation dynamics of Rydberg states in an ultracold gas for a realistically large number of atoms, which is well beyond the capacity of a full quantum calculation. We can reproduce the Rydberg blockade effect observed previously and also its effect on the atom counting statistics, but in addition we have identified an antiblockade effect due to the Autler-Townes splitted Rydberg population. We predict that this antiblockade effect can be seen in an experiment with a gas trapped in an optical lattice created by a CO_2 laser since the antiblockade is robust even against a large number of lattice defects. In the (realistic) limit of a very small upper Rabi frequency ω we could show that the formation of the double or single peak structure in the Rydberg population is determined by a universal parameter. It allows a simple navigation in parameter space consisting of the two Rabi frequencies, the decay rate of the intermediate level and the pulse length, to achieve the desired peak structure in the single-atom Rydberg excitation probability.

This work was partially supported by NSF through a grant for ITAMP.

[1] M. D. Lukin, M. Fleischhauer, R. Cote, L. M. Duan, D. Jaksch, J. I. Cirac, and P. Zoller, Phys. Rev. Lett. **87**, 037901 (2001).
[2] D. Tong, S. M. Farooqi, J. Stanojevic, S. Krishnan, Y. P. Zhang, R. Cote, E. E. Eyler, and P. L. Gould, Phys. Rev. Lett. **93**, 063001 (2004).
[3] K. Singer, M. Reetz-Lamour, T. Amthor, L. G. Marcassa, and M. Weidemüller, Phys. Rev. Lett. **93**, 163001 (2004).
[4] T. Cubel-Liebisch, A. Reinhard, P. R. Berman, and G. Raithel, Phys. Rev. Lett. **95**, 253002 (2005).
[5] F. Robicheaux and J. V. Hernandez, Phys. Rev. A **72**, 063403 (2005).
[6] C. Ates, T. Pohl, T. Pattard, and J. M. Rost, J. Phys. B **39**, L233 (2006).
[7] C. Ates, T. Pohl, T. Pattard, and J. M. Rost (to be published).
[8] R. M. Whitley and C. R. Stroud, Jr., Phys. Rev. A **14**, 1498 (1976).
[9] W. Li, P. J. Tanner, and T. F. Gallagher, Phys. Rev. Lett. **94**, 173001 (2005).
[10] We have taken the values of $\mu_{sp}\mu_{sp'}$ and δ_0 from [9] for $n = 48$ ($\mu_{sp}\mu_{sp'} = 843\,800$ a.u., $\delta_0 = -0.0378$ a.u.) and adapted them to other Rydberg levels by appropriate scaling in n [9].
[11] S. Friebel, C. D'Andrea, J. Walz, M. Weitz, and T. W. Hänsch, Phys. Rev. A **57**, R20 (1998).
[12] The pulse length is yet assumed to be shorter than the lifetime of the shortest-lived Rydberg state considered in this work ($\tau_{40s} \approx 80$ μs), see: A. L. de Oliveira, M. W. Mancini, V. S. Bagnato, and L. G. Marcassa, Phys. Rev. A **65**, 031401 (2002).